

Journal of Optoelectronical Nanostructures



Winter 2024 / Vol. 6, No. 1

Research Paper

Thin-film perovskite solar cell incorporating Gaussian and incremental gratings to optimize light absorption

Seyed Mohsen Mohebbi Nodez¹, Masoud Jabbari¹*, Ghahraman Solookinejad²

- ¹Department of Electrical Engineering, Marvdasht Branch, Islamic Azad University, Marvdasht, Iran.
- ²Department of Physics, Marvdasht Branch, Islamic Azad University, Marvdasht, Iran.

Received: Revised: Accepted: Published:

Use your device to scan and read the article online



DOI:

Kevwords:

Thin-Film Solar Cells Perovskite, Gratings, Gaussian, Absorption, Plasmonic, Scattering.

Abstract:

This paper proposes a Gaussian grating to enhance light absorption in perovskite thin-film solar cells. As gratings are effective structures for trapping light within the active layer of a cell, a two-dimensional Gaussian grating with a rectangular structure is considered for the front surface of the cell. Finite element method results demonstrate that the Gaussian grating significantly increases light absorption in a 0.5 micrometer thick cell within the visible and near-infrared range compared to a cell without a grating and a cell with a conventional or incremental grating. The average absorption of the cell with a Gaussian grating is 85.6%, representing a 90% increase compared to the reference cell. Moreover, the short-circuit current density and efficiency were found to be 28.3 mA/cm² and 34.8%, respectively, indicating increases of 74% and 74.8%, respectively, compared to the reference cell. The proposed cell structure shows promise for improved light-to-electricity conversion.

Citation: Seyed Mohsen Mohebbi Nodez, Masoud Jabbari, Ghahraman Solooki nejad Thin-film perovskite solar cell incorporating Gaussian and incremental gratings to optimize light absorption. **Journal of Optoelectronical Nanostructures.** 2024; 1 (1): 48-58

*Corresponding author: Masoud Jabbari

1. INTRODUCTION

Given the global energy crisis and the urgent need for sustainable technologies, solar cells (SCs) have emerged as a viable option for converting solar energy into electricity [1]. Extensive research has been conducted annually on various generations of solar cells. Economic considerations also play a crucial role in the adoption of SCs, as they must be more cost-effective compared to other energy sources such as fossil fuels, nuclear energy, geothermal, tidal, and others [2]. A significant portion of the costs is associated with the fabrication process of SCs. For instance, the production of thick silicon-based SCs requires substantial amounts of raw materials and energy to achieve the necessary purity [3]. In contrast, thin-film solar cells can be produced through deposition processes, which are much more energy-efficient and material-friendly. Therefore, thin-film technology seems to be a suitable solution to address these challenges. Moreover, various materials such as CIGS, CdTe, amorphous silicon, and perovskite can be used in this technology, and extensive research has been conducted to develop thin-film SCs [4]. Despite their economic advantages, thin-film solar cells (TFSCs) exhibit lower power conversion efficiencies due to limited light absorption. This is because the active layer thickness is less than a few micrometers, preventing the absorption of a significant portion of incident photons. This effect is more pronounced for long-wavelength photons, which can be reflected from the back surface without being absorbed [5]. To improve the efficiency of SCs, various approaches have been proposed, including intermediate bandgap SCs [6, 7], hot carriers [8, 9], and light trapping techniques [10]. Light trapping enhances absorption by employing specific structures and geometries such as front and back surface gratings [11], plasmonic nanostructures [12-14], and nanowires [15, 17]. Grating structures, in particular, induce changes in the propagation vector of incident light due to periodic variations in the refractive index, thereby increasing light trapping [18]. Furthermore, these structures increase the optical path length through scattering and diffraction, thereby enhancing the probability of photon interaction with atoms in the active layer. One-dimensional and two-dimensional periodic and quasi-periodic gratings have been employed on the front, back, or both surfaces of the cell [19-21]. For instance, Chen et al. investigated enhanced light absorption in amorphous silicon by incorporating aluminum-copper plasmonic nanowire networks on both sides. The top pair of networks, coupled with an anti-reflection coating, is responsible for minimizing reflection losses and enhancing absorption of short-wavelength visible light in the active layer. The bottom pair enhances the absorption of longwavelength photons in the active layer. As a result, amorphous silicon, which exhibits low absorption for long wavelengths, can now absorb broadband light

from 670 to 1000 nm with an average absorption rate of over 70% and an improved current density of 21.9 mA/cm² [22]. Zhang Chen et al. investigated nanostructured plasmonic metals, including copper, gold, and silver, as back reflectors for thin-film amorphous silicon solar cells. Solar cells with these reflectors demonstrated excellent light trapping in the long-wavelength region. By combining hybrid cavity resonances, horizontal modes, and surface plasmon resonances, more incident light is coupled into the active layer. Compared to reference cells, the proposed structures with plasmonic reflectors exhibit lower parasitic absorptions with distinct absorption distributions. Simulation and experimental results indicate that the silver reflector performs the best with a promising efficiency of 7.28% and a current density of 13.76 mA/cm² [23].Bozzola et al. presented the effect of front surface microstructures on light trapping in amorphous silicon thin-film solar cells. The structured coatings provide strong broadband improvements in the generated current due to reduced light reflection at short wavelengths and increased optical path length for long wavelengths. As a result, in the structures analyzed in this study, significant increases in efficiencies (up to 14.5%) and currents (up to 21.7%) were achieved compared to reference cells [24]. Kamal et al. investigated the enhancement of light absorption in hydrogenated amorphous silicon solar cells using dielectric nanostructures made of silicon nitride. Silicon nitride acts as an anti-reflective coating, reducing light reflection from the cell surface. The customized design of the anti-reflective coating in the form of nanostructured dielectric layers resulted in a 15.2% increase in short-circuit current compared to the reference cell [25]. All proposed networks have a regular, periodic, or quasi-periodic structure that increases the absorption rate of the active layer. In this paper, a grating structure with a Gaussian distribution along the x-axis is presented and simulated using the finite element method (FEM). Gaussian gratings trap light by scattering it into the active layer, resulting in higher light absorption compared to solar cells with conventional gratings. The highest average absorption, short-circuit current density, and efficiency are 85.6%, 34.8 mA/cm², and 28.3%, respectively. This represents a 90% increase in average absorption, 73% increase in current density, and 74.8% increase in efficiency compared to solar cells without gratings.

2. THE PROPOSED STRUCTURE

Figure.1 shows the schematic of the proposed solar cell with a Gaussian grating on its back surface. The proposed solar cell consists of a 250 nm thick silver back reflector, a 500 nm thick perovskite active layer, and a Gaussian distributed grating with width wg, height hg, and period P. The refractive indices of silver

and perovskite are also taken from reference [26]. Equation (1) shows the distribution function used for the proposed Gaussian gratings, where n represents the number of gratings, which is chosen as 9 in this paper, nave represents the average value of the gratings and is equal to 5, hg0 represents the height of the central grating, hg0 = 250 nm, and P0 is the period of the structure and is considered to be 300 nm, and ζ is also a constant that determines the width of the gratings. [27] In Figure 2, the Gaussian grating distribution is plotted for different values of ζ . It is observed that as the value of ζ increases from 0.2 to 0.7, the height of the side gratings increases.

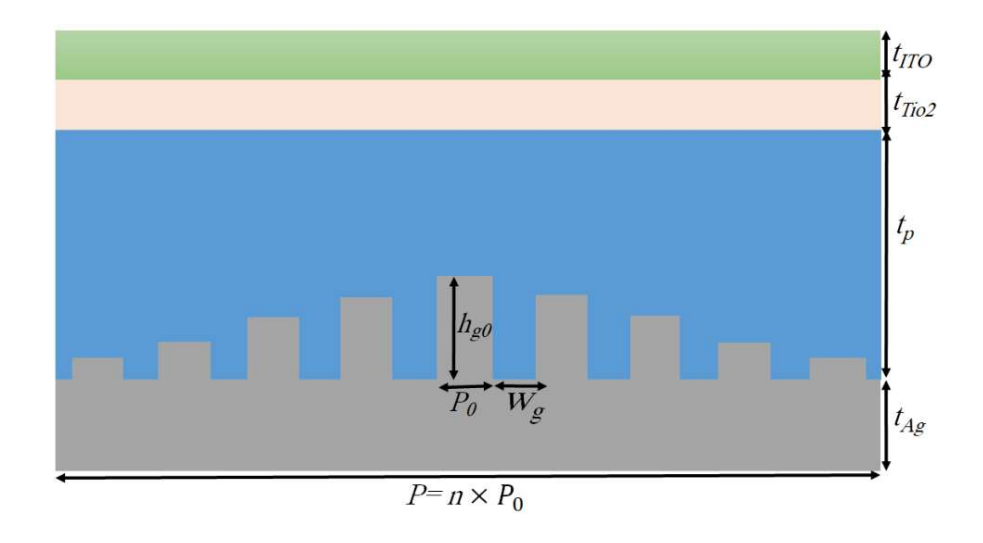
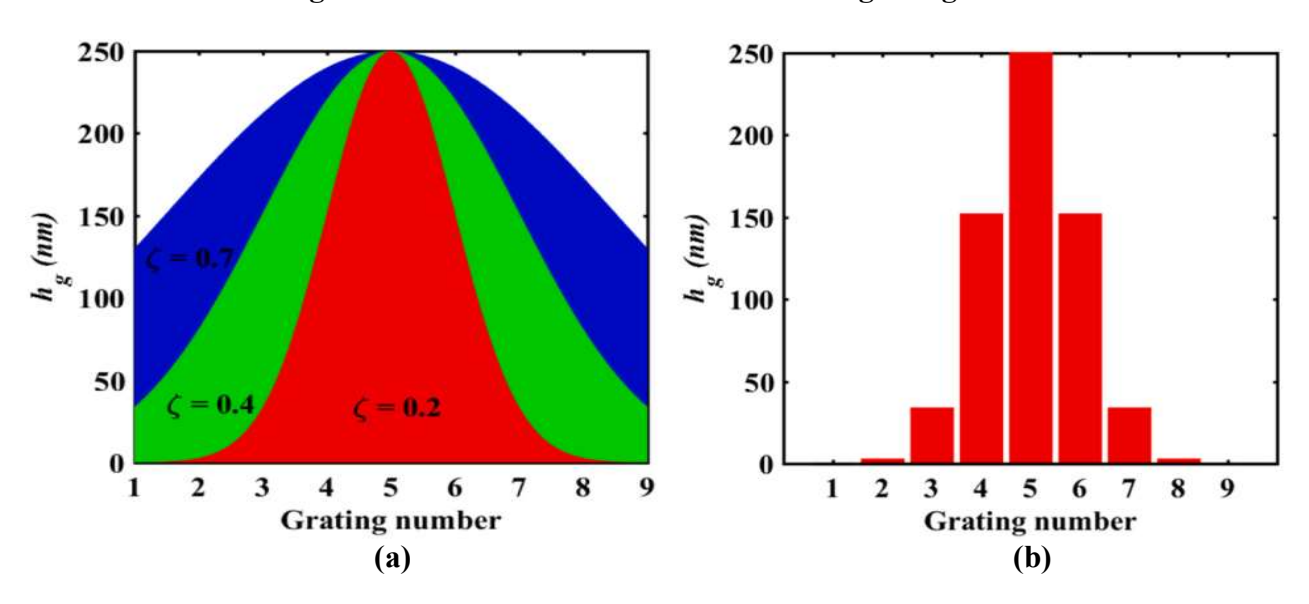


Fig. 1: The schematic of SC with Gaussian gratings.



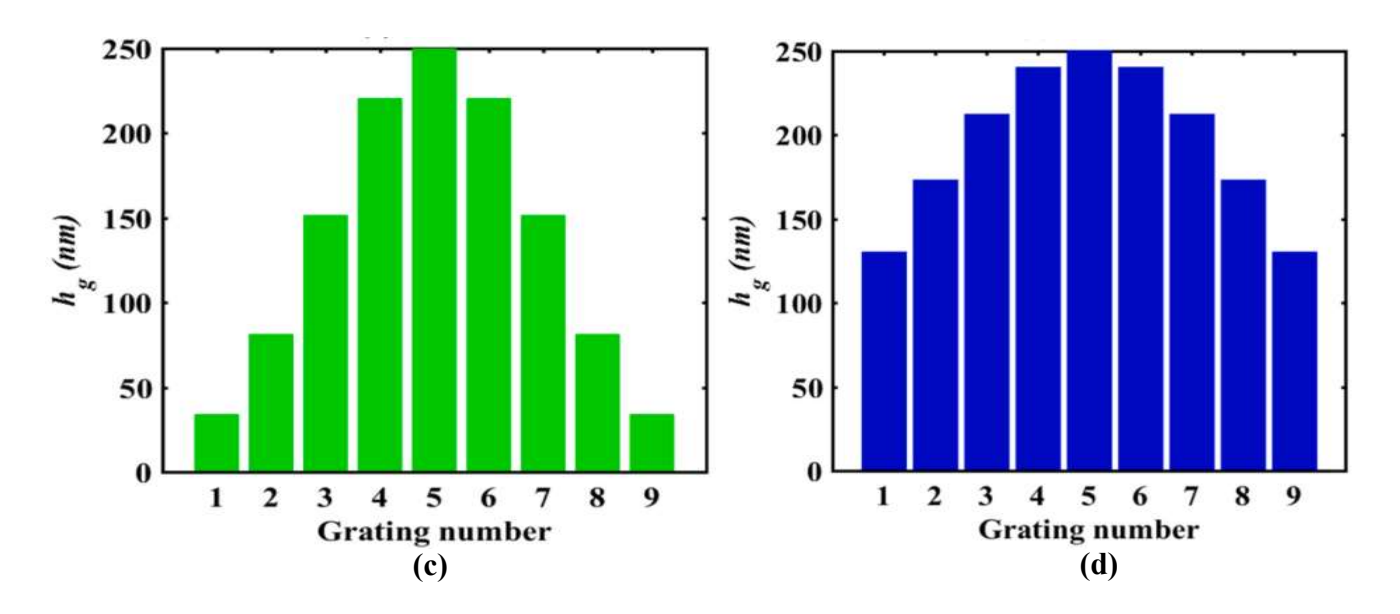


Fig. 2. a) Gaussian function distribution profile according to the number of gratings and for different ζ of 0.1, 0.3, and 0.6; Gaussian grating distribution diagram according to: b) $\zeta = 0.1$, c) $\zeta = 0.3$ and d) $\zeta = 0.6$.

3. MATHEMATICAL FORMULATIONS

The figure shows how the parameter ζ affects the shape of the Gaussian curve and consequently the grating structure. A crucial parameter that plays a significant role in the design of solar cells is the plot of absorption versus the wavelength of incident light, which indicates the cell's ability to absorb light. Light absorption in each region of the cell can be calculated using equation (2) [27]:

$$h_g = h_{g0} exp \left(\frac{-\left(\frac{n}{n_{ave}} - 1\right)}{2\zeta^2} \right)^2 \tag{1}$$

$$A(\lambda) = \frac{\varepsilon_0 \omega}{2} \frac{\varepsilon i''(\lambda)}{P_{in}(\lambda)} \int_{V} |E(\lambda)|^2 dV$$
 (2)

Where ω is the angular frequency, λ is the wavelength, $\epsilon 0$ is the permittivity of free space, $\epsilon'(\lambda)$ is the imaginary part of the dielectric constant, $E(\lambda)$ is the wavelength-dependent electric field intensity, and $Pin(\lambda)$ is the solar irradiance. On the other hand, as a result of light irradiation, charge carriers are generated, which lead to the creation of a photocurrent, so that the short-circuit current density and the open-circuit voltage of the cell can also be calculated from the following relations [27]:

$$J_{SC} = \frac{q}{hc} \int_{300nm}^{1000nm} \lambda A(\lambda) I(\lambda) d\lambda$$
 (3)

$$V_{OC} = \frac{KT}{q} ln \left(\frac{J_{ph}}{J_0} + 1 \right) \tag{4}$$

Where q is the electron charge, h is the Planck constant, c is the speed of light, K is the Boltzmann constant, T is the ambient temperature, Jph is the generated photocurrent, J0 is the dark saturation current, and $I(\lambda)$ is the AM1.5 irradiance reaching the Earth. Finally, the following formula can be used to calculate the power conversion efficiency:

$$\eta = \frac{J_{SC}V_{OC}FF}{P_{in}} \tag{5}$$

Where FF is the fill factor and Pin is the solar irradiance, which is equal to 100 milliwatts per square centimeter [27].

4. RESULTS

4.1.OPTIMAL DIMENSION

In this section, we present the simulation results of the proposed structure using the finite element method (FEM). Simulations include a cell without a grating (reference cell), cells with conventional and Gaussian gratings. In Figure 3, the absorption and reflection spectra of three types of solar cells with an active layer thickness of 500 nm are shown. Figure 3(a) corresponds to the reference cell, which has an average absorption of 47.5%. It is observed that this cell has a weak absorption due to more light reflection from its surface. In this case, we observe absorption peaks at wavelengths of 743 nm and 883 nm. In order to increase its absorption, a conventional grating with a width and height of 100 nm and a period of 300 nm was used and its absorption spectrum is shown in Figure 3(b). It is observed that by applying the conventional grating, the amount of absorption in the visible region has increased significantly and the average absorption has reached 62.8%, which represents a 44.3% increase compared to the reference cell. The reason for this is the reduction of reflection from the cell surface and acting as an anti-reflection layer. The reason for the reduction in reflection is due to the scattering of light by the gratings. Thus, it can be concluded that by reducing the amount of reflection, more light scattering can be achieved in the active region, and as a result, absorption increases. In Figure 3(c), the amount of light absorption for hg0 = 250 nm, wg = 250 nm, and ζ = 0.3 is plotted. It is observed that the presence of a Gaussian grating causes maximum light absorption in the visible

wavelengths, and the average absorption reaches 85.6%, which represents a 90% increase compared to the reference cell. For a better comparison of the absorption spectra of the three types of cells, the absorption plot based on their wavelength is shown in Figure 3(d). For the cell with Gaussian gratings, in addition to a significant increase in the visible region, we observe the formation of absorption peaks at longer wavelengths in the infrared region, which is due to the presence of gratings with different heights that scatter longer wavelengths into the active layer [26].

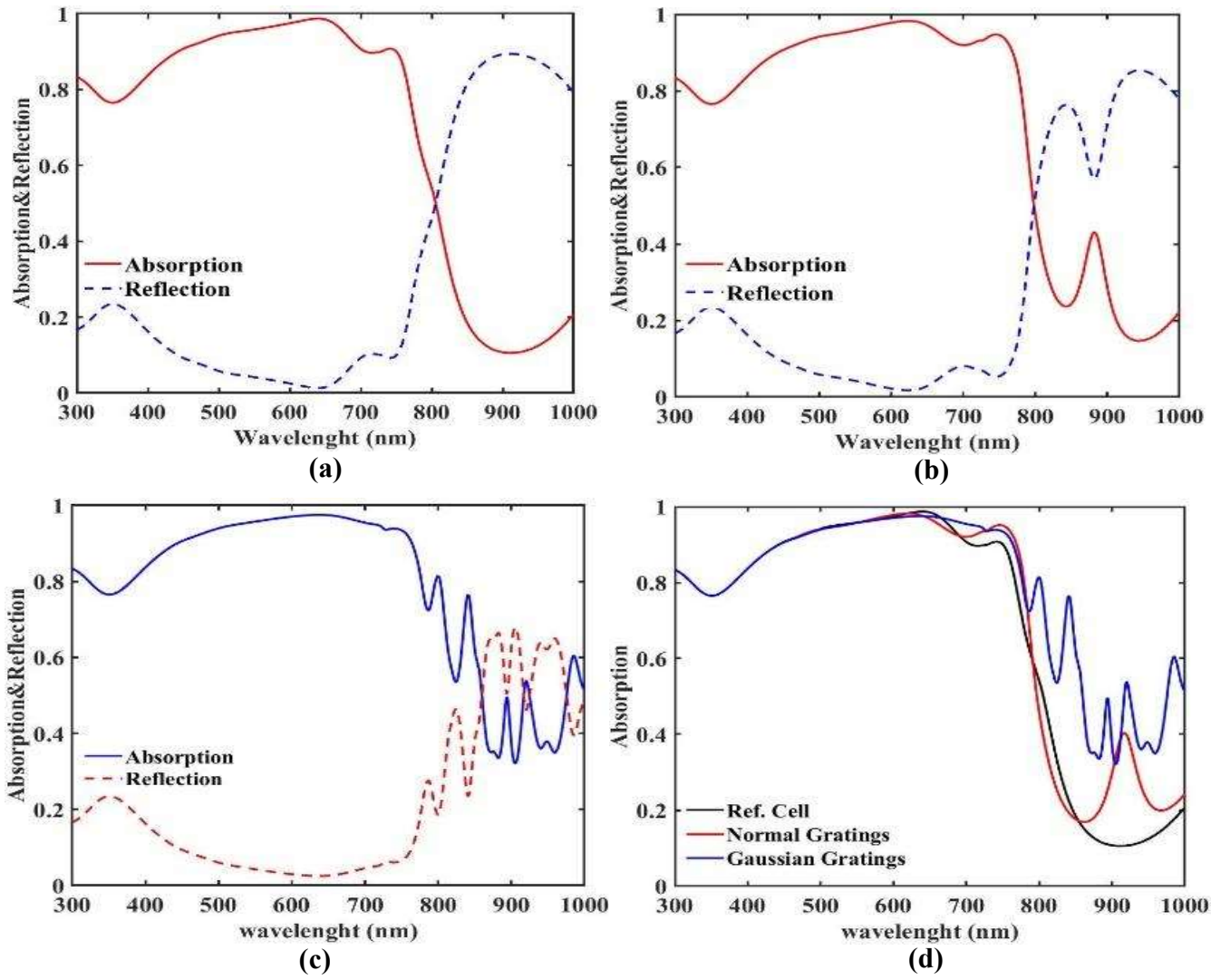


Fig. 3. Absorption and reflection spectra vs. wavelength for: a) reference cell, b) cell with normal gratings with wg = 100 nm, hg = 100 nm, and P0 = 300 nm, and c) cell with Gaussian grating for hg0 = 250 nm, wg = 250 nm, P0 = 300 nm, and $\zeta = 0.4$; d) Absorption spectra in terms of wavelength for all three types of SCs.

The reason for this is the reduction of reflection from the cell surface, acting as an anti-reflection layer. The decrease in reflection is due to the scattering of light by the gratings. Thus, it can be concluded that by reducing reflection, more light scattering can be achieved in the active region, leading to increased absorption. In Figure 3(c), the light absorption for hg0 = 250 nm, wg = 250 nm, and ζ = 0.3 is plotted. The presence of a Gaussian grating results in maximum light absorption in the visible wavelength range, with an average absorption reaching 85.6%, representing a 90% increase compared to the reference cell. For a better comparison of the absorption spectra of the three cell types, the absorption plot based on wavelength is shown in Figure 3(d). For the cell with Gaussian gratings, in addition to a significant increase in the visible region, absorption peaks are observed at longer wavelengths in the infrared region. This is due to the presence of gratings with varying heights that scatter longer wavelengths into the active layer [26]. In Table 1, the average absorption, short-circuit current density, and efficiency for all three types of cells are shown. It is observed that the short-circuit current density and efficiency increased from 21.6 mA/cm² and 11.8% in the reference cell to 26.37 mA/cm² and 15.4% in the cell with conventional gratings. Meanwhile, the values of current density and efficiency for the cell with Gaussian gratings are 34.8 mA/cm² and 28.3%, respectively, indicating an increase of 73% and 74.8% compared to the reference cell [26,27].

Table 1: Average absorption of the SC without grating and SCs with normal gratings and Gaussian gratings.

Gratings type	No	Normal	Gaussian
	gratings	gratings	gratings
Average absorption (%)	50.32	54.97	68.33
Short circuit current density	21.6	26.37	34.8
(mA/cm2)			
Efficiency (%)	22.35	23.31	28.3

The results indicate that increasing the grating size generally leads to a decrease in average absorption. This is attributed to the reduced efficiency of conventional gratings in scattering light into the cell, coupled with increased parasitic losses in silver gratings, which ultimately reduces net absorption. To enhance light scattering and absorption, Gaussian gratings with varying heights, widths, and ζ values, as described in [26], were introduced. Figures 4(b) and 4(a) show the average absorption for different widths and heights relative to different ζ values. The highest absorption is obtained at a width of 150 nm and a height of 250 nm for $\zeta = 0.3$.

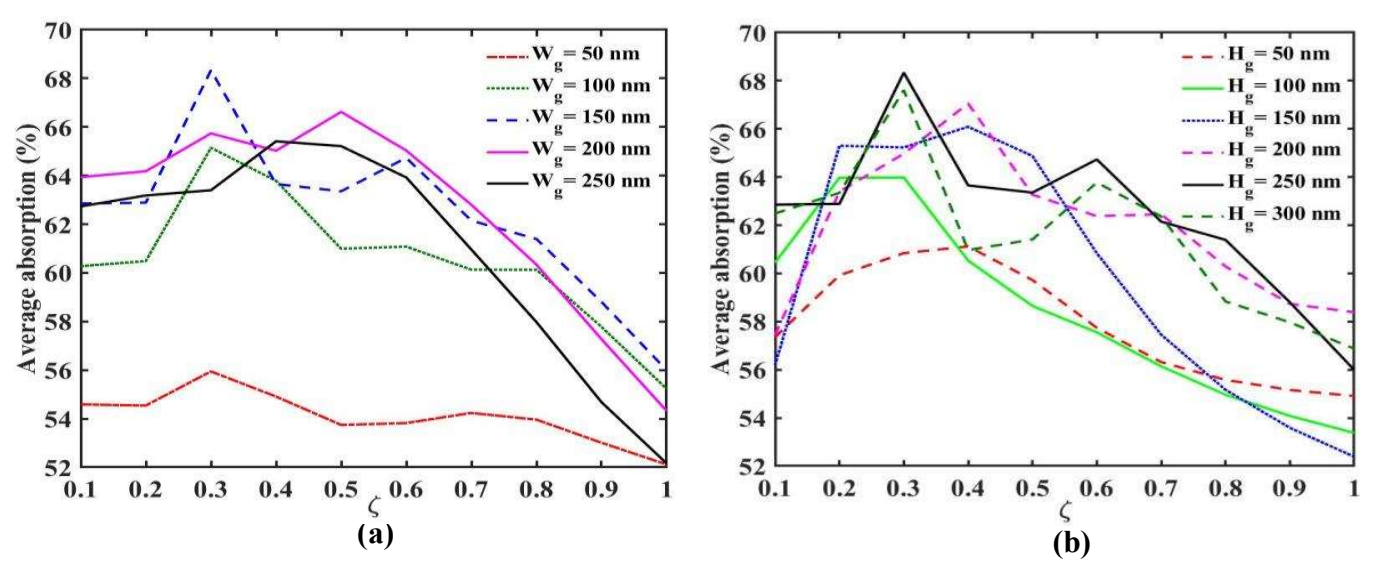


Figure .4. The average absorption versus hg with different wg for SC the average absorption according to the ζ for different wg.

To investigate the absorption mechanism in the proposed solar cells, the electric field intensity for the reference cell and cells with conventional and Gaussian gratings is shown in Figure 5. Figure 5-a shows the electric field intensity for the reference cell at a wavelength of 741 nm, corresponding to the absorption peak. It is observed that the electric field has a uniform distribution, and darker regions are formed due to resonances. Due to the effect of light on the back reflector and its reflection into the active layer, constructive interference with the incident wave is formed, and absorption increases. In Figures 5(b) and 5(c), the electric field distribution profiles for the cell with conventional gratings at a wavelength of 835 nm and the cell with Gaussian gratings at a wavelength of 823 nm are shown, respectively. It is observed that both gratings have changed the distribution of field profiles within the active regions and formed darker spots, indicating light confinement and increased electric field intensity. On the other hand, due to the dependence of absorption on it, absorption increases[28].

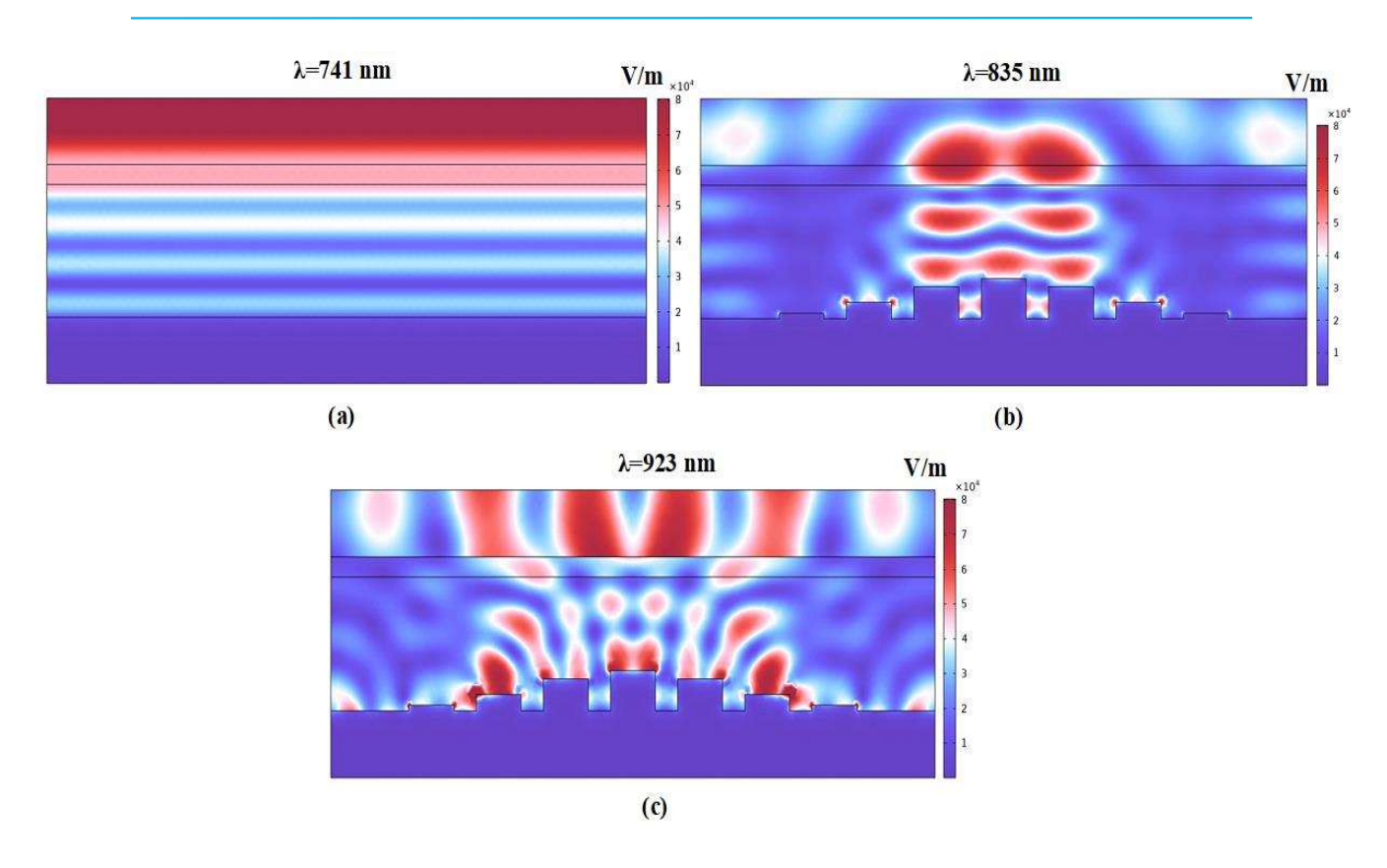


Fig.5. Electric field distribution profile for the: reference cell, b) cell with normal gratings and c) cell with Gaussiangratings at determined wavelengths.

In the following, we investigate the effect of parameters ζ , height hg0, and width wg in solar cells with Gaussian gratings. The absorption spectra as a function of wavelength for values of 0.1, 0.3, 0.6, and 1 are shown in Figure 6(a). It is observed that when ζ is equal to 0.3, the absorption curve has the highest absorption value compared to the others. This is due to the ability to trap light by reducing light reflection from the cell surface, and it can be said that this height is the optimal dimension. In Figure 6(b), the absorption spectra as a function of wavelength for different widths wg in the range of 50 to 250 nm are shown. In Figure 6(c), the effect of height hg0 on absorption is plotted. Gaussian gratings with a height of 250 nm show better absorption compared to other heights. It is observed that with increasing the width of the gratings, the absorption spectra show significant changes and their values increase, so that the highest absorption is observed at wg = 250 nm. The reason for this is the significant reduction in light reflection from the cell surface due to its scattering inside the cell. In other words, gratings with a width of 250 nm have the ability to couple more light into the active layer. In Figure 6(c), the average absorption spectrum as a function of ζ and for different heights hg0 is shown. It is observed that with increasing ζ from 0.1

to 1, the average absorption also increases, and at $\zeta = 0.3$, the highest average absorption of 85.6% is obtained. However, for values greater than 0.3, the average absorption decreases [26,29].

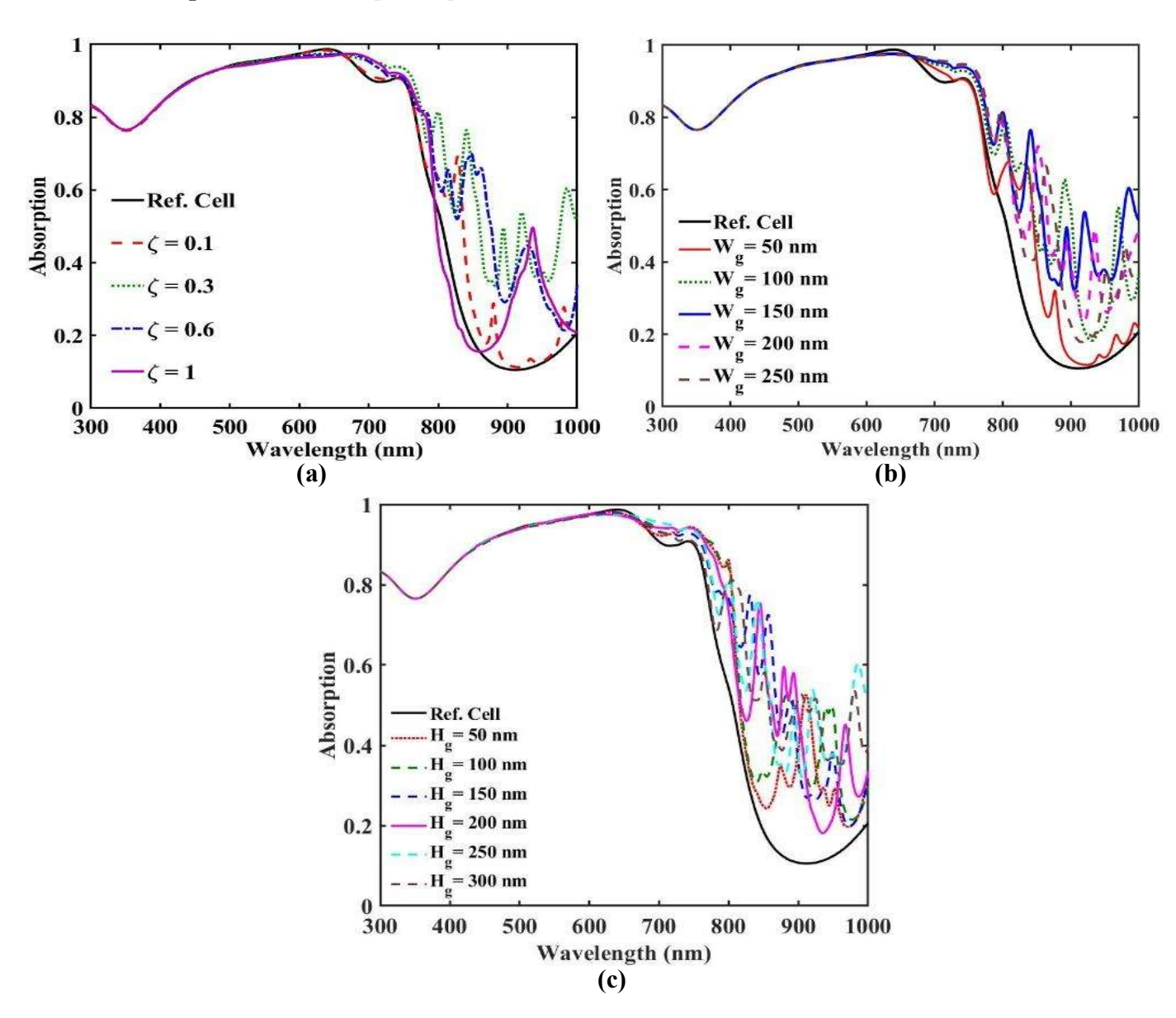


Fig. 6. Absorption spectrum in terms of wavelength for: a) different ζ , b) different wg, c) different hg.

To investigate the effect of changing the grating width and ζ on absorption, all widths from 50 to 300 nm were swept, and the absorption spectra for $\zeta = 0.1$, $\zeta = 0.3$, and $\zeta = 1$ are shown in Figure 7. It is observed that the absorption value shows significant changes with variations in both width and ζ . This is because both parameters play an important role in reducing light reflection as an anti-reflection layer. Near-complete absorption occurred for $\zeta = 0.3$, which is better than the other two values, and an increase in absorption is observed for widths greater than 150 nm, as indicated by the darker regions [26,30].

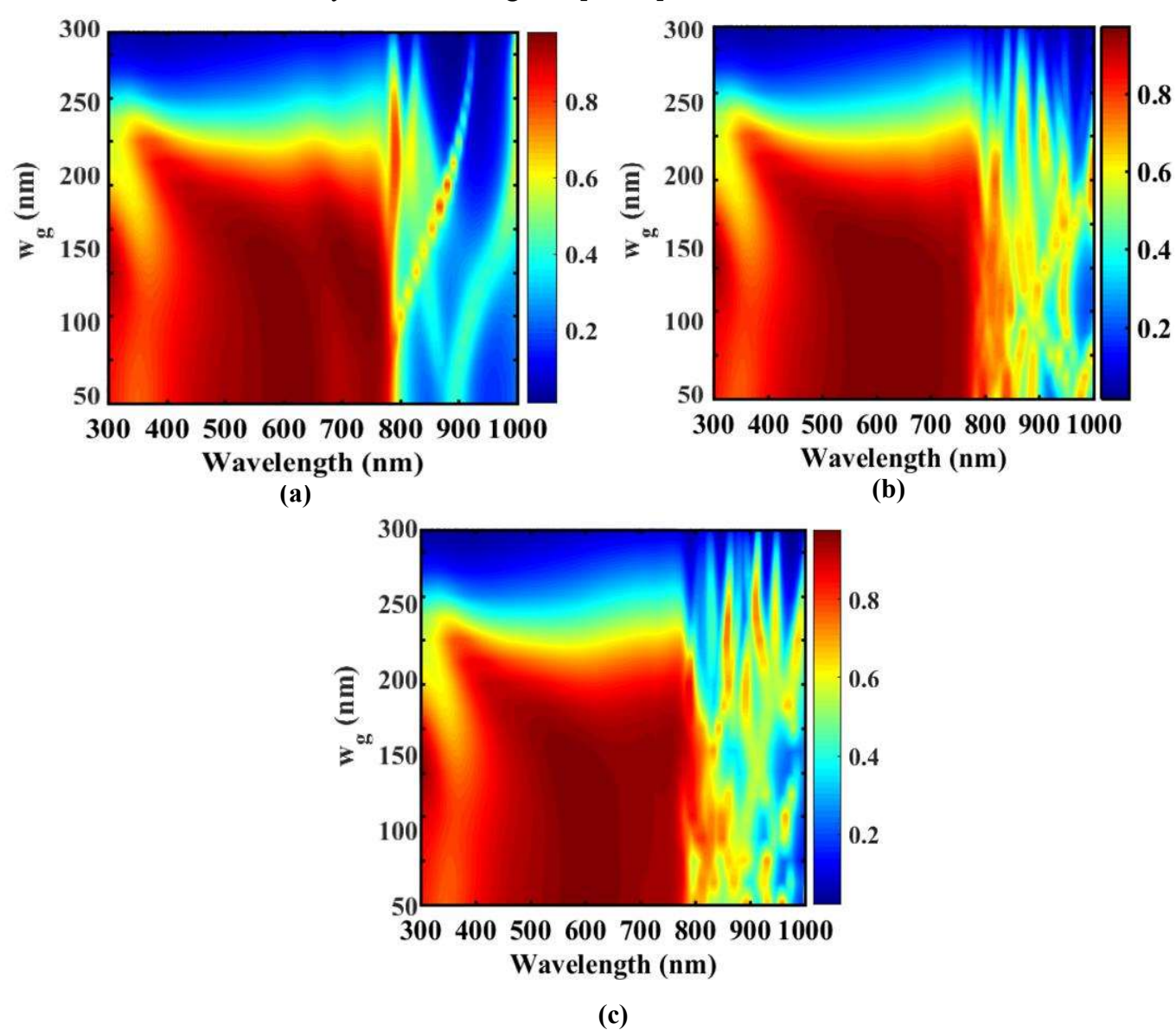
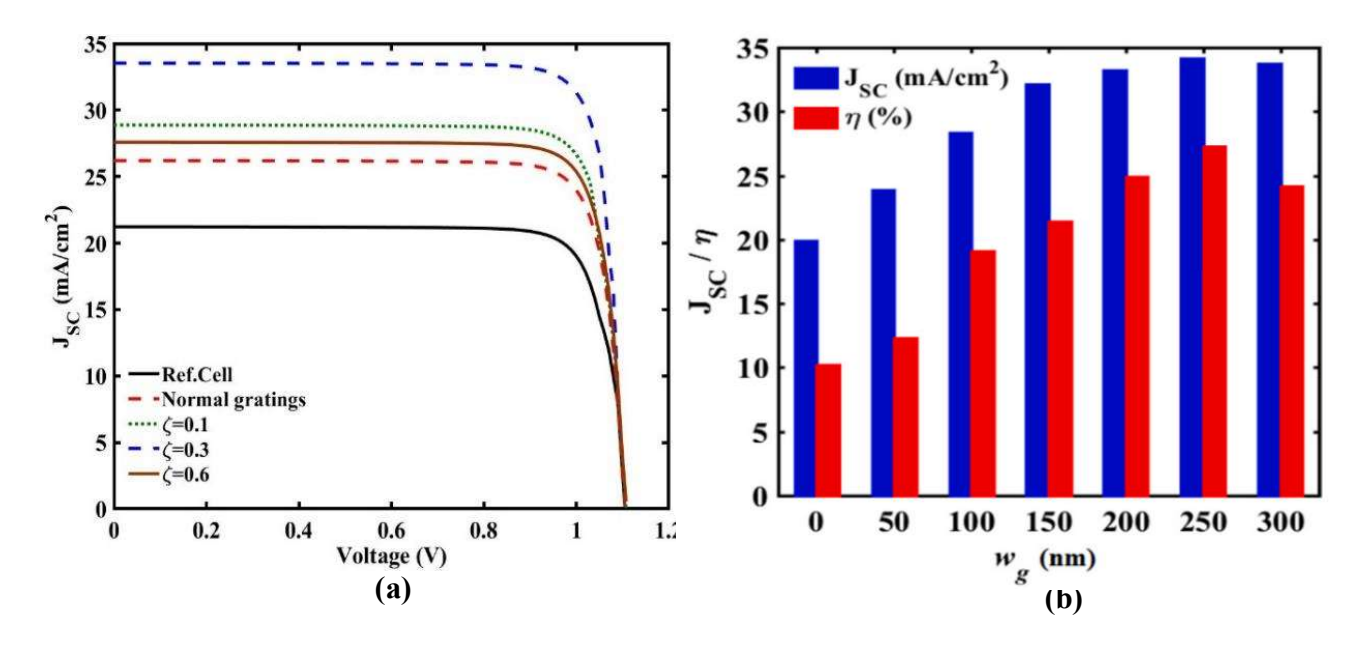


Fig. 7. Absorption spectra in terms of wavelength and gratings width for: a) $\zeta = 0.1$, b) $\zeta = 0.3$, and c) $\zeta = 1$.

4.2. CURRENT ABSORPTION

Short-circuit current density and efficiency are two important parameters for analyzing the performance of solar cells. In Figures 8(a) and (b), the values of short-circuit current density and efficiency as a function of ζ for different hg0 values are shown, respectively. As can be seen, in each of the hg0 values, with increasing ζ , both current density and efficiency increase and reach a maximum value, and then show a decreasing trend. The reason for this is the changes in the amount of light absorption, since the current density is directly related to the absorbed light. The highest values of current density, 34.8 mA/cm², and efficiency, 28.3%, are obtained for $\zeta = 0.3$ and hg0 = 250 nm in Figure 8(a). In Figure 8(b), the effect of changing wg on both current density and efficiency is shown. In this case, $\zeta = 0.3$ and hg0 = 250 nm are selected, and it is observed that at wg = 250 nm, the maximum values of current density and efficiency occur. In Figure 8(c), the absorption spectrum as a function of wavelength and angle of incidence from 0 to 85 degrees for solar cells with Gaussian gratings is shown. It is observed that up to an angle of 45 degrees, the absorption for wavelengths less than 800 nm has values higher than 0.7, and therefore it can be said that Gaussian gratings perform well at oblique angles of incidence, and it is also clear in this figure that the Gaussian grating has an average of more than 87% for angles less than 40 degrees.



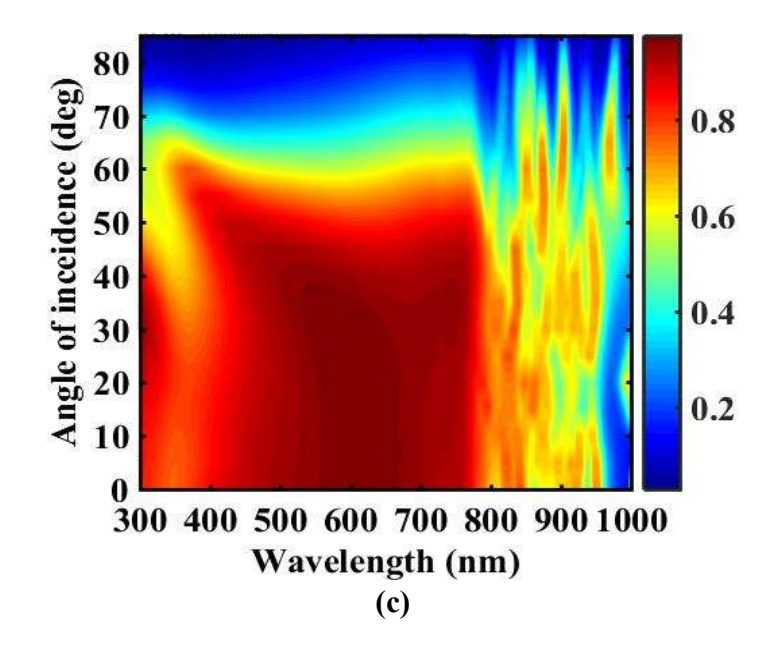


Fig. 8. a) Short circuit current density diagrams and efficiency in terms of grating width, and b) Current-voltage characteristic for reference cell, c) Absorption spectrum of cell with Gaussian gratings in terms of wavelength and radiation angle.

5.CONCLUSION

Due to their unique structure, gratings scatter light into the active region, thereby increasing light absorption. Various types of grating structures, including onedimensional and two-dimensional gratings with regular and random distributions, have been presented in different works. In this paper, the effect of Gaussian gratings on increasing absorption in the active layer of perovskite solar cells was investigated. To this end, Gaussian gratings were considered on the front surface of the cell, and the absorption rate in the active region was calculated and compared with the absorption rate of the reference cell and the cell with a conventional grating. FEM simulation results showed that these types of gratings, due to their special geometry, effectively trap sunlight within the active layer and significantly increase the amount of absorption in the visible and near-infrared regions of the solar spectrum. The findings show that the average absorption of cells with Gaussian gratings is 85.6%, which represents a 90% increase compared to the absorption of reference cells. On the other hand, the short-circuit current density and efficiency were obtained as 34.8 mA/cm² and 28.3%, respectively, indicating an increase of 74% and 74.8% compared to the reference cell. Thus, a

newly designed solar cell with higher absorption and higher efficiency was presented, promising the emergence of a cell with the ability to convert more and more light into electricity.

References

- [1] E.R.W. Mac Queen, M. Liebhaber, J. Niederhausen, M. Mews, C. Gersmann, S. Jackle, K. Lips, *Crystalline silicon solar cells with tetracene interlayers: the path to siliconsinglet fission heterojunction devices*, Mater. Horiz. 5 (6) (2018) 1065–1075, Available:doi:10.1039/C8MH00853A.
- [2] C. Battaglia, A. Cuevas, S.D. Wolf, *High-efficiency crystalline silicon solar cells status and perspectives*, Energy Environ. Sci. 9 (5) (2016) 1552–1576, Available:doi: https://doi.org/10.1039/C5EE03380B.
- [3] H. Naim, D.K. Shah, A. Bouadi, M.R. Siddiqui, M.S. Akhtar, C.Y. Kim, *An in-depth optimization of thickness of base and emitter of ZnO/Si heterojunction-based crystalline silicon solar cell*: a simulation method, J. Electron. Mater. 51 (2) (2022) 586–593, Available:doi: https://doi.org/10.1007/s11664-021-09341-5.
- [4] S. Cao, D. Yu, Y. Lin, C. Zhang, L. Lu, M. Yin, D. Li, Light propagation in flexible thin-film amorphous silicon solar cells with nanotextured metal back reflectors, ACS Appl. Mater. Interfaces 12 (23) (2020) 6184–26192, Available:doi: https://doi.org/10.1021/acsami.0c05330.
- [5] D.L. McGott, C.P. Muzzillo, C.L. Perkins, J.J. Berry, K. Zhu, J.N. Duenow, M.O. Reese, *3D/2D passivation as a secret to success for polycrystalline thin-film solarcells*, Joule 5 (5) (2021) 1057–1073, Available:doi: https://doi.org/10.1016/j.joule.2021.03.015.
- [6] J. Ramanujam, D.M. Bishop, T.K. Todorov, O. Gunawan, J. Rath, R. Nekovei, A. Romeo, *Flexible CIGS, CdTe and a-Si: H based thin film solar cells: a review*, Prog. Mater. Sci. 110 (2020) 100619, Available:doi: https://doi.org/10.1016/j.
- [7] X. Zhaopeng, H. Huangfu, L. He, J. Wang, D. Yang, J. Guo, H. Wang, Light-trapping properties of the Si inclined nanowire arrays, Opt. Commun. 382 (2017) 332–336, Available:doi: https://doi.org/10.1016/j.optcom.2016.08.018.

- [8] M.A. Elrabiaey, M. Hussein, M.F.O. Hameed, S.S. Obayya, *Light absorption enhancement in ultrathin film solar cell with embedded dielectric nanowires*, Sci. Rep. 10 (1) (2020) 17534, Available:doi: https://doi.org/10.1038/s41598-020-74453-7.
- [9] R. Ren, Z. Zhong, Enhanced light absorption of silicon solar cells with dielectric nanostructured back reflector, Opt. Commun. 417 (2018) 110–114, Available:doi: https://doi.org/10.1016/j.optcom.2018.02.051.
- [10] Y.H. Jang, Y.J. Jang, S. Kim, L.N. Quan, K. Chung, D.H. Kim, *Plasmonic solar cells:from rational design to mechanism overview*, Chem. Rev. 116 (24) (2016)14982–15034, Available:doi: https://doi.org/10.1021/acs.chemrev.6b00302.
- [11] F. Enrichi, A. Quandt, G.C. Righini, *Plasmonic enhanced solar cells: summary of possible strategies and recent results*, Renew. Sustain. Energy Rev. 82 (2018) 2433–2439, Available:doi: https://doi.org/10.1016/j.rser.2017.08.094
- [12] L. Long, Y. Yang, L. Wang, Simultaneously enhanced solar absorption and radiative cooling with thin silica micro-grating coatings for silicon solar cells, Sol. Energy Mater. Sol. Cell 197 (2019) 19–24, Available:doi: https://doi.org/10.1016/j.solmat.2019.04.006
- [13] T. Sun, H. Shi, L. Cao, Y. Liu, J. Tu, M. Lu, F. Zhang, *Double grating high efficiency nanostructured silicon-based ultra-thin solar cells*, Results Phys.19(2020)103442, Available: doi: https://doi.org/10.1016/j.rinp.2020.103442.
- [14] C. Heine, R.H. Morf, Submicrometer gratings for solar energy applications, Appl. Opt. 34 (14) (1995) 2476–2482, https://doi.org/10.1364/AO.34.002476.
- [15] S. Elewa, B. Yousif, M.E.A. Abo-Elsoud, *Improving efficiency of perovskite solar cell using optimized front surface nanospheres grating*, Appl. Phys. A 127 (11)(2021) 1–14, Available:doi: https://doi.org/10.1007/s00339-021-05019-1
- [16] P. Tillmann, B. Bl" asi, S. Burger, M. Hammerschmidt, O. Hohn, "C. Becker, K. J" ager, *Optimizing metal grating back reflectors for III-V-on-silicon multijunction solarcells*, Opt. Express 29 (14) (2021) 22517–22532, Available:doi: https://doi.org/10.1364/OE.426761.
- [17] R. Chen, Z. Hu, Y. Ye, J. Zhang, Z. Shi, Y. Hua, *An anti-reflective 1D rectangle grating on GaAs solar cell using one-step femtosecond laser fabrication*, Opt. Lasers Eng. 93 (2017) 109–113, Available:doi: https://doi.org/10.1016/j.optlaseng.2017.01.017.

- [18] W. Lan, Y. Wang, J. Singh, F. Zhu, *Omnidirectional and broadband light absorption enhancement in 2-D photonic-structured organic solar cells*, ACS Photonics 5 (3)(2018) 1144–1150, Available:doi: https://doi.org/10.1021/acsphotonics.7b01573.
- [19] A.P. Amalathas, M.M. Alkaisi, *Nanostructures for light trapping in thin film solar cells*, Micromachines 10 (9) (2019) 619, Available:doi: https://doi.org/10.3390/mi10090619
- [20] K.X. Wang, Z. Yu, V. Liu, Y. Cui, S. Fan, Absorption enhancement in ultrathin crystalline silicon solar cells with antireflection and light-trapping nanocone gratings, Nano Lett. 12 (3) (2012) 1616–1619, Available:doi: https://doi.org/10.1021/nl204550q.
- [21] H. Zheng, Y. Yu, R. Wu, S. Wu, S. Chen, K. Chen, *Period-mismatched sine dualinterface grating for optical absorption in silicon thin-film solar cells*, Applied Optics. 59 (33) (202) 10330–10338. Available:doi: https://doi.org/10.1364/AO.408812.
- [22] K. Chen, N. Zheng, S. Wu, J. He, Y. Yu, H. Zheng, *Effective light trapping in c-Si thin-film solar cells with a dual-layer split grating*, Appl. Opt. 60 (33) (2021)10312–10321, Available:doi: https://doi.org/10.1364/AO.443307.
- [23] J. Zhang, Z. Yu, Y. Liu, H. Chai, J. Hao, H. Ye, *Dual interface gratings design for absorption enhancement in thin crystalline silicon solar cells*, Opt. Commun. 399 (2017) 62–67, Available:doi: https://doi.org/10.1016/j.optcom.2017.04.062.
- [24] Bozzola, M. Liscidini, L.C. Andreani, *Broadband light trapping with disordered photonic structures in thin-film silicon solar cells, Prog.*Photovolt.: Res. Appl. 22 Available:doi: https://doi.org/10.1002/pip.2385.
- [25] Elshorbagy, M. H., Abdel-Hady, K., Kamal, H., & Alda, J. (2017). *Broadband anti-reflection coating using dielectric Si3N4 nanostructures*. Application to amorphous-Si-H solar cells. Optics Communications, Available:doi: 390, 130-136.
- [26] Mohebbi Nodez, S. M., Jabbari, M., & Solookinejad, G. (2023). *Absorption enhancement of Perovskite Solar Cells using multiple Gratings*. Physica Scripta. Available: doi:10.1088/1402-4896/ace2f6.
- [27] Hamid Heidarzadeh (2019), *Incident light management in a thin silicon solar cell using a twodimensional grating according a Gaussian distribution*. Available: doi:10.1016/j.solener.2019.07.099.

- [28] Mojtaba Shahraki, Majid Ghadrdan, *Efficiency Improvement of InGaP/SiGe tandem solar cell using Si0.18Ge0.82 graded buffer regions*. Journal of Optoelectronical Nanostructures. Available: 10.30495/jopn.2024.33226.1313
- [29] Behrooz Vaseghi; Ghasem Rezaei; Nasim Mohammadi; Shakiba Mardani, *Terahertz Resonance Fluorescence of a Spherical Gaussian Quantum Dot*. Journal of Optoelectronical Nanostructures. Available: 10.30495/jopn.2024.33360.1316
- [30] Mohsen Nasrolahi; Ali farmani; Ashkan Horri; Hossein Hatami, FDTD Analysis of a High-sensitivity refractive index sensing based on Fano resonances in a plasmonic planar split-ring resonators. Journal of Optoelectronical Nanostructures.

Available: 10.30495/jopn.2024.33499.1321